Journal of ELECTRONIC MATERIALS, Vol. 37, No. 1, 2008
DOI: 10.1007/s11664-007-0262-x

Special Issue Paper

Characterization of Interfacial Reaction Layers Formed Between Sn-3.5Ag Solder and Electroless Ni-Immersion Au-Plated Cu Substrates

HAN-BYUL KANG,[1] JEE-HWAN BAE,[1] JAE-WOOK LEE,[1] MIN-HO PARK,[1] JEONG-WON YOON,[2] SEUNG-BOO JUNG,[2] and CHEOL-WOONG YANG[1,3]

1.—School of Advanced Materials Science and Engineering, Center for Nanotubes and Nanostructured Composites, Sungkyunkwan University, Suwon 440-746, Korea. 2.—School of Advanced Materials Science and Engineering, Sungkyunkwan University, Suwon 440-746, Korea. 3.—e-mail: cwyang@skku.edu

The interfacial reaction between a eutectic Sn-3.5wt.%Ag solder and an electroless nickel–immersion gold-plated Cu substrate during reflow was examined by transmission electron microscopy (TEM). During the initial reflowing, the amorphous, electroless Ni (P)-plated layer crystallized into two P-rich Ni layers: a $Ni_{12}P_5$ + Ni_3P mixed upper layer and a Ni_3P lower layer. No ternary Ni-Sn-P layer was observed in the initial stage. After subsequent reflow for 60 s, a ternary Ni_2SnP layer (containing a small amount of the Ni_3P phase) was formed between the Ni_3Sn_4 and P-rich Ni layers (Ni_3P + $Ni_{12}P_5$ + Ni).

Key words: Solder, transmission electron microscopy, electroless nickel–immersion gold

INTRODUCTION

Lead (Pb)-free solder has attracted considerable attention in electronic materials research due to the recent health and environmental concerns with lead.[1–20] Of the many different solder alloys that have been proposed as potential Pb-free solders, the alloy families of Sn-Ag and Sn-Ag-Cu have shown the greatest promise.[4,11] In addition to solder, printed circuit boards (PCBs) and component surface finishes also need to be Pb-free. The selection of the appropriate substrate metallization plays an important role in the development of a reliable packaging technology. Cu has been widely used in the under bump metallization (UBM) of a chip and in substrate metallization for chip packaging. However, the reliability of this solder joint has raised serious concern, due to the rapid formation of a Cu-Sn intermetallic compound (IMC) at the Sn-based solder/Cu interface.[21] The formation of a thin IMC layer is needed to achieve good metallurgical bonding, but excessive IMC growth adversely affects the mechanical reliability of ball-grid-array (BGA) and flip-chip solder joints. Because this problem of IMC overgrowth is exacerbated in the case of Pb-free solders, Ni, particularly in the form of electroless nickel–immersion gold (ENIG), has been widely used as a surface finish layer on the metal bond pad for flip-chip and BGA solder bumps, due to its low cost and simple processing.[11,20] Besides the original properties of solder and surface finish materials, the interfacial reaction between the solder and substrate is another important parameter for determining joint reliability.[21] In the case of electroless Ni (P) plating, the presence of P makes the reaction between Sn and Ni (P) more complicated than that between Sn and Cu or pure Ni. In addition to the existence of Ni-containing IMCs, the reliability of the solder joints is decreased by the formation of additional layers, such as ternary Ni-Sn-P and P-rich Ni (Ni_2P, $Ni_{12}P_5$ and Ni_3P).[11,19] Furthermore, these layers are quite thin.[11] Therefore, many studies have examined the interfacial reaction of SnAg/ENIG.[17,20,22] Various analysis techniques, such as scanning electron

(Received March 15, 2007; accepted June 26, 2007; published online: September 22, 2007)

microscopy (SEM), electron probe microanalyzer (EPMA), and transmission electron microscopy (TEM), have been used to examine interfacial reaction. Of these, TEM equipped with analytical attachments offers the most complete tool for characterizing the formation of these additional layers. However, solders are typically soft, while IMCs tend to be quite hard and brittle, which has limited the level of success in preparing solder samples for TEM analysis. This study evaluated the interfacial reaction between eutectic Sn-3.5wt.%Ag solder and ENIG-plated Cu substrate during reflowing at 255°C, using an ultramicrotome and TEM.

EXPERIMENTAL PROCEDURES

The composition of the BGA solder balls used in this study was Sn-3.5Ag (in wt.%) and their diameters were 500 μm. The substrate was a flame retardant (FR4) PCB, which was plated with Au and Ni (P) layers using an ENIG surface finish to a thickness of 0.15 μm and 5 μm, respectively. The electroless Ni (P) layer contained approximately 15 at.% phosphorous (P) due to the use of hypophosphite in the chemical reduction of Ni ions. The solder balls were bonded to the pads during the reflow process using a rosin mildly activated (RMA)-type flux in a reflow machine (RF-430-N2, Japan Pulse Laboratory Co. Ltd., Japan) at a maximum temperature of 255°C for 3 s and 60 s. The preheating time was approximately 60 s at 160°C. After the reflow process, the samples were cooled to room temperature.

The microstructure and chemical composition were examined with a TEM equipped with an energy dispersive X-ray spectrometer (EDS). The cross-sectional samples for the TEM were prepared with an ultramicrotome (RMC MT7000). Using this method, we obtained TEM samples with uniform thickness, less contamination, and a large observable area. Each flat polished specimen (approximately 100 μm in thickness) was embedded with Epofix (Struers) in an embedding mold. After being trimmed, the embedded sample was sectioned at 0.3 mm/s window speed, a 5° bevel angle, and a 40 nm sectioning thickness with a diamond knife (Druker). The sectioned samples were collected onto a 3 mmΦ Mo grid. The sample was examined with a high-resolution (HR)-TEM (JEM-2100F, Jeol Co. Ltd.) equipped with a scanning transmission electron microscope (STEM)/EDS. In addition, a nanobeam electron diffraction (NBED) technique was used for the crystallographic confirmation of the phases formed at the joint.

RESULTS AND DISCUSSION

Figure 1 shows a TEM micrograph of the Sn-3.5Ag/ENIG interface after reflowing at 255°C for 3 s and the selected area diffraction (SAD) patterns obtained from four reaction layers: electroless Ni (P) plated layer (layer A), P-rich Ni layer (layers B and C) and Ni_3Sn_4 IMC layer (layer D). Based on the TEM image contrast, it is apparent that the P-rich layer between the Ni_3Sn_4 IMC and the electroless Ni (P) is composed of two reaction layers rather than one. The lower layer B next to the

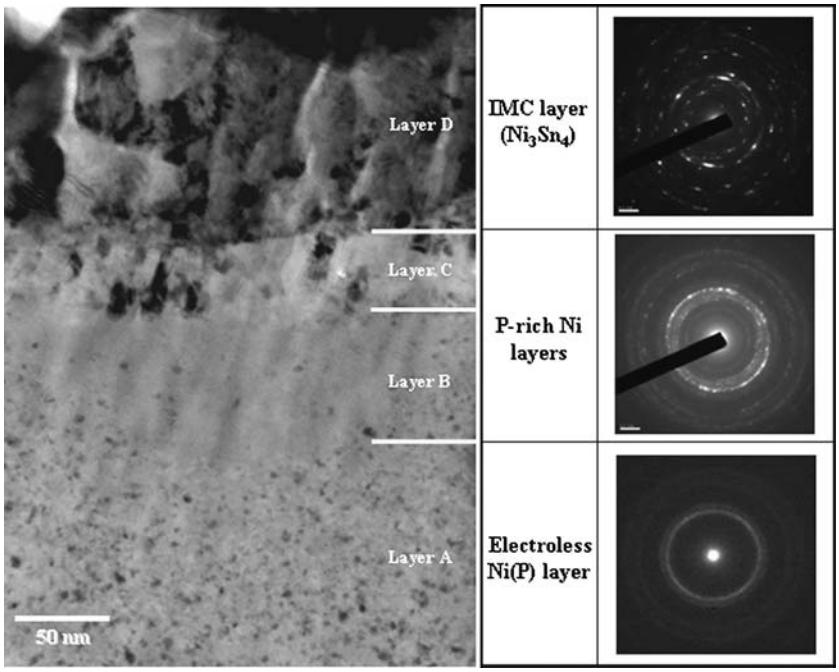

Fig. 1. Cross-sectional TEM micrograph of the Sn-3.5Ag/ENIG interface reflowed at 255°C for 3 s and selected area diffraction (SAD) patterns obtained from electroless Ni (P) plated layer (layer A), P-rich Ni layer (layers B and C) and Ni_3Sn_4 IMC layer (layer D). The P-rich layer between the Ni_3Sn_4 IMC and the electroless Ni (P) was composed of two reaction layers rather than one.

electroless Ni (P) shows a relatively homogeneous gray contrast, while the upper layer C next to the Ni_3Sn_4 IMC shows a dappled (gray and dark) contrast. The SAD pattern of the electroless Ni (P) plated layer indicates diffused halo rings, which is typical of an amorphous structure. In contrast, diffraction pattern of the P-rich Ni layer that formed in front of the electroless Ni (P) layer consists of a Debye ring superimposed with spots, which suggests that the P-rich Ni layer contains fine polycrystals of a Ni-P compound.

STEM/EDS analysis confirmed that no Au-containing phase or Au layer was present at any position of the interface. Layers B and C contained relatively more P than did the bottom layer. In addition, no P was detected in the Ni_3Sn_4 IMC layer. Considering the compositional ratio between Ni and P, layers B (positions 7–9 in Fig. 2) and C (positions 4–6 in Fig. 2) are most likely to be $Ni_{12}P_5$ or Ni_3P phases. NBED was used to identify the phases in the P-rich Ni layers. Figure 3 shows the NBED patterns obtained from the P-rich Ni layers

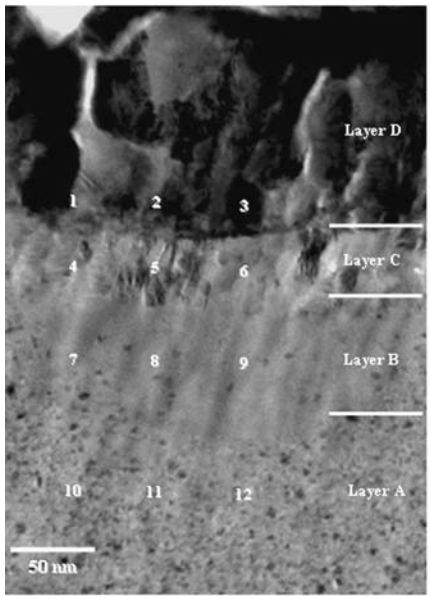

Position	Ni	P	Sn
	at.%	at.%	at.%
1	47.30 ± 2.41	-	52.70 ± 1.19
2	41.80 ± 2.21	-	58.20 ± 1.05
3	46.04 ± 1.77	-	53.96 ± 1.10
4	69.12 ± 0.93	30.88 ± 1.77	-
5	72.23 ± 1.28	27.27 ± 2.44	-
6	72.05 ± 0.94	27.95 ± 1.78	-
7	77.33 ± 0.77	22.67 ± 1.46	-
8	76.23 ± 0.74	23.77 ± 1.40	-
9	76.80 ± 0.72	23.20 ± 1.37	-
10	85.59 ± 0.62	14.41 ± 1.17	-
11	82.46 ± 0.69	17.54 ± 1.30	-
12	86.28 ± 0.65	13.72 ± 1.22	-

Fig. 2. STEM micrograph of the Sn-3.5Ag/ENIG interface reflowed at 255°C for 3 s and the results of EDS analysis (electron probe size 1 nm). Considering the compositional ratio between Ni and P, the layers B (positions 7–9) and C (positions 4–6) are likely to be phases based on either $Ni_{12}P_5$ or Ni_3P.

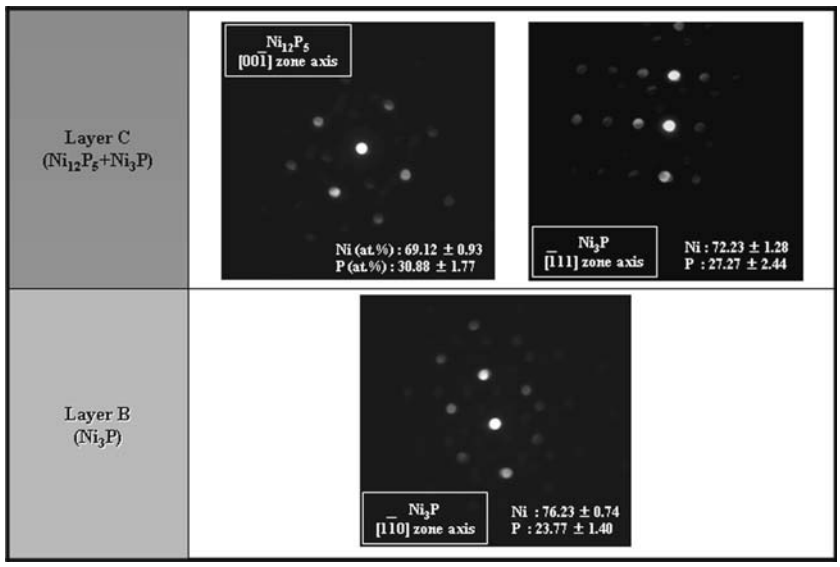

Fig. 3. NBED patterns obtained from STEM/EDS analysis of the positions shown in Fig. 2. The upper P-rich Ni layer is $Ni_{12}P_5$ (NBED pattern measured at position 4) and Ni_3P (NBED pattern measured at position 5). The lower P-rich Ni layer is Ni_3P (NBED pattern measured at position 8).

next to the Ni_3Sn_4 IMC in Fig. 2. NBED analysis confirmed that the upper P-rich Ni layer (layer C) is composed of $Ni_{12}P_5$ and Ni_3P. The lower P-rich Ni layer (layer B) is mainly composed of Ni_3P. This result is consistent with the STEM/EDS results.

During the reflow process, the uppermost Au flash layer was completely dissolved into the molten solder, leaving a Ni (P) layer exposed to the molten solder. In addition, Sn atoms in the solder reacted with the Ni atoms at the solder/Ni (P) interface, causing the formation of Ni_3Sn_4 IMC at the interface. Owing to the consumption of Ni to form Ni_3Sn_4 IMC, P was expelled to the remaining Ni-P layer to form these P-rich Ni layers. This phenomenon is generally known as "solder reaction-assisted crystallization".[23] The mechanism is based on the preferential dissolution of Ni from the Ni (P) layer, which leads to an increase in the P content in the upper part of the Ni (P) layer and subsequent Ni_3P formation. NBED/EDS analysis confirmed that Ni_3P and $Ni_{12}P_5$ were formed in the P-rich Ni layer in the initial reflow process. Therefore, Ni_3P was the phase of the initial reaction, and $Ni_{12}P_5$ might also have been formed in the initial reflow process. It is believed that this $Ni_{12}P_5$ phase was formed between the IMC layer and the Ni (P) plated layer due to the rapid diffusion of Ni. The large amount of Ni is diffused into the solder layer at the initial reflow process, forming IMCs at the interface. The Ni concentration is significantly lower at the upper most region of the P-rich Ni layer (the region immediately below the solder). $Ni_{12}P_5$ containing a relatively low concentration of Ni could be formed. Therefore, the upper P-rich layer contains $Ni_{12}P_5$ (layer C in Fig. 1). In addition, the ternary Ni-Sn-P layer, which is generally recognized as the layer between the interfacial IMC and the P-rich Ni layers, was not observed in the initial stage after reflow for 3 s.

The joint was then reflowed at 255°C for a prolonged time (60 s) in order to determine the microstructural and compositional changes in the Sn-3.5Ag/ENIG joint. Figure 4 shows the cross-sectional TEM micrograph of the interface reflowed for 60 s. A significantly different interfacial reaction was observed in the specimen. There are two distinct layers between the interfacial Ni_3Sn_4 IMC and Ni (P) layers: the lower thick layer (light gray, approximately 750 nm in thickness) and an upper thin layer (dark gray, approximately 200 nm in thickness). The difference in the contrast indicates that the top layer contains heavier elements (Sn) than the lower one does. EDS analysis showed that the dark gray region (layer C in Fig. 4) is composed of Ni, Sn and P, while the light gray region (layer B in Figs. 4 and 5) contains Ni and P only. Electron-diffraction pattern analysis (Fig. 6) combined with the EDS analysis confirmed the bottom layer (layer B) to be composed of Ni_3P, $Ni_{12}P_5$ and Ni, while the top layer (layer C) is a mixture of Ni_2SnP and Ni_3P. These layers do not consist of a single phase but,

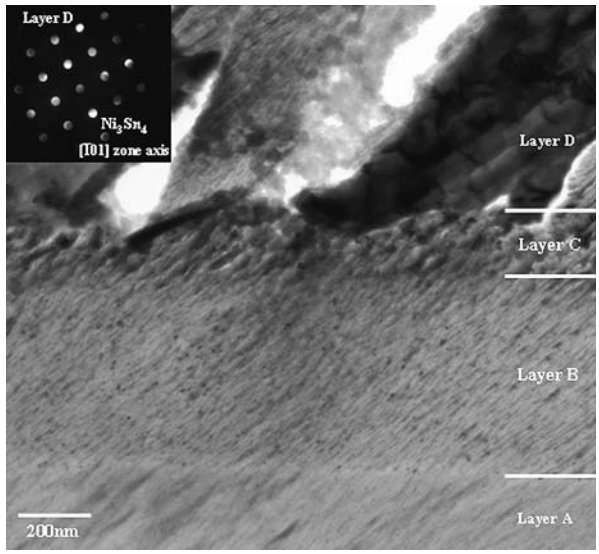

Fig. 4. Cross-sectional TEM micrograph of the Sn-3.5Ag/ENIG interface reflowed at 255°C for 60 s and the NBED patterns obtained from the Ni_3Sn_4 IMC layer (layer D). A markedly different interfacial reaction was observed from the specimen. There were two distinct layers between the interfacial Ni_3Sn_4 IMC and Ni (P) layers.

rather, are composed of two or three phases. Indeed, the main phases of the layers B and C were Ni_3P and Ni_2SnP, respectively.

The ternary Ni-Sn-P phase has been reported in a few studies examining the Sn-Ag/Ni (P) system.[15–20] Hwang et al. examined the interfacial reaction between the Sn-3.5Ag solder and Au (0.06 μm)/Ni-6wt.%P (5 μm) plated layer at a reflow temperature of 230°C for 40 s and reported that Ni_3SnP formed on top of the Ni_3P layer in Sn-3.5Ag/Ni-P joints.[20] Lin and Duh reported the transformation of Ni_2P-Ni_2SnP as a result of the in-diffusion of Sn.[15] Although the precise reason for the formation of this Ni_2SnP layer is unclear, it is presumably related to the transformation of an upper P-rich Ni layer ($Ni_{12}P_5$ + Ni_3P) that had formed in the previous reaction.

Two possibilities for the formation of Ni_2SnP can be deduced. Figure 7 shows a schematic diagram of this process. As shown in the figure, the Ni_2SnP phase can be formed by a reaction between the $Ni_{12}P_5$ phase and internally diffused Sn because $Ni_{12}P_5$ is formed at the upper P-rich Ni layer before the formation of Ni_2SnP (A $\rightarrow$ B in Fig. 7). However, $Ni_{12}P_5$ is a meta-stable phase that is easily transformed into other Ni-P compounds.[15,24] Therefore, $Ni_{12}P_5$ converts to Ni_2P as a result of continuous Ni diffusion. From the Ni-P binary phase diagram,[24] Ni-P compounds appear in the form of Ni_3P, Ni_5P_2, $Ni_{12}P_5$ and Ni_2P in sequence with decreasing Ni content. It is expected that Ni_2P should be the next phase to be formed after $Ni_{12}P_5$. Therefore, with the successive diffusion of Ni, $Ni_{12}P_5$ can be transformed to Ni_2P between the IMC and the lower P-rich Ni layer (A $\rightarrow$ α in Fig. 7). Although

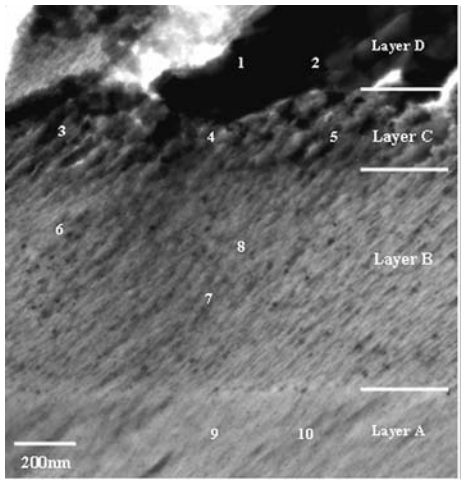

Position	Ni	P	Sn
	at.%	at.%	at.%
1	46.04 ± 1.77	-	53.96 ± 1.10
2	46.09 ± 2.74	-	53.91 ± 1.36
3	59.33 ± 1.72	12.63 ± 1.33	28.04 ± 0.99
4	60.37 ± 1.69	15.46 ± 1.40	24.17 ± 0.90
5	51.37 ± 1.97	15.25 ± 1.85	33.38 ± 1.07
6	72.05 ± 0.94	27.95 ± 1.78	-
7	77.33 ± 0.77	22.67 ± 1.46	-
8	76.23 ± 0.74	23.77 ± 1.40	-
9	85.59 ± 0.62	14.41 ± 1.17	-
10	86.28 ± 0.65	13.72 ± 1.22	-

Fig. 5. The results of STEM/EDS analysis (electron probe size 1 nm). The dark gray region (layer C in Fig. 4) is composed of Ni, Sn and P, while the light gray region (layer B in Fig. 4) is composed of Ni and P only.

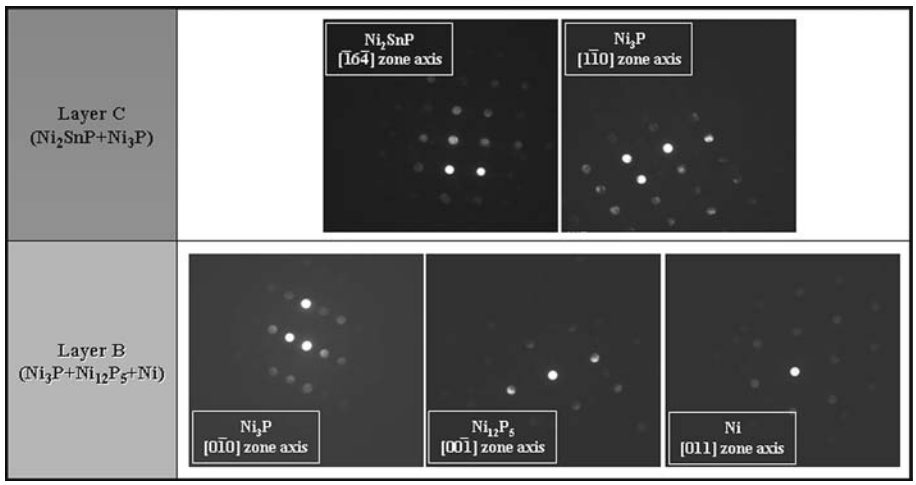

Fig. 6. NBED patterns obtained from layers B and C in Fig. 5. The bottom layer (layer B) is composed of Ni_3P, $Ni_{12}P_5$ and Ni, while the top layer (layer C) is a mixture of Ni_2SnP and Ni_3P.

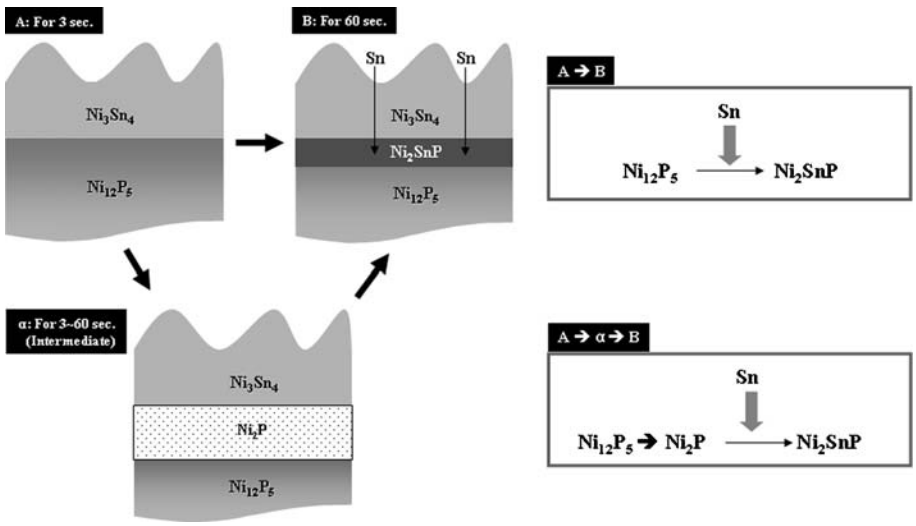

Fig. 7. Schematic diagram for the formation of the Ni_2SnP ternary phase.

the Ni_2P phase was not detected in this study, it might be possible to form a Ni_2P phase through an intermediate (3–60 s) reflow reaction. Therefore, it is possible that the Sn atoms diffused into Ni_2P to form Ni_2SnP (A $\rightarrow$ α $\rightarrow$ B in Fig. 7). These results are in agreement with those reported by Lin and Duh.

CONCLUSIONS

This study examined the interfacial reaction between eutectic Sn-3.5wt.%Ag solder and an ENIG-plated Cu substrate during reflow, using a TEM. During the initial reflow for 3 s, the amorphous, electroless Ni (P) plated layer crystallized into two P-rich Ni layers: a $Ni_{12}P_5$ + Ni_3P mixed upper layer and a Ni_3P lower layer. In addition, the ternary Ni-Sn-P layer, which is generally recognized as a layer formed between the interfacial IMC layer and the P-rich Ni layer, was not observed in the initial stage. After a prolonged reflow reaction for 60 s, a ternary Ni_2SnP layer (containing a small amount of Ni_3P) was formed between the Ni_3Sn_4 and P-rich Ni layers (Ni_3P + $Ni_{12}P_5$ + Ni).

ACKNOWLEDGEMENTS

This work was supported by Grant No. RTI04-03-04 from the Regional Technology Innovation Program of the Ministry of Commerce, Industry and Energy (MOCIE) and, in part, by a grant from the Korea Science and Engineering Foundation (KOSEF) through the Center for Nanotubes and Nanostructured Composites (CNNC).

REFERENCES

1. K. Zeng and K.N. Tu, *Mater. Sci. Eng. R.* 38, 55 (2002).
2. M. Abtew and G. Selvaduray, *Mater. Sci. Eng. R.* 27, 95 (2000).
3. J.W. Yoon, S.W. Kim, and S.B. Jung, *Mater. Trans.* 45, 727 (2004).
4. K. Suganuma, *Curr. Opin. Solid State Mater. Sci.* 5, 55 (2001).
5. J.W. Yoon, S.W. Kim, J.M. Koo, D.G. Kim, and S.B. Jung, *J. Electron. Mater.* 33, 1190 (2004).
6. J.W. Yoon and S.B. Jung, *J. Mater. Res.* 21, 1590 (2006).
7. J.W. Yoon, J.H. Lim, H.J. Lee, J. Joo, W.C. Moon, and S.B. Jung, *J. Mater. Res.* 21, 3196 (2006).
8. M.N. Islam, Y.C. Chan, and A. Sharif, *J. Mater. Res.* 19, 2897 (2004).
9. W.C. Luo, C.E. Ho, J.Y. Tsai, Y.L. Lin, and C.R. Kao, *Mater. Sci. Eng., A* 396, 385 (2005).
10. C.H. Wang and S.W. Chen, *Acta Mater.* 54, 247 (2006).
11. S.W. Kim, J.W. Yoon, and S.B. Jung, *J. Electron. Mater.* 33, 1182 (2004).
12. J.W. Jang, D.R. Frear, T.Y. Lee, and K.N. Tu, *J. Appl. Phys.* 88, 6359 (2000).
13. S.J. Wang and C.Y. Liu, *Scripta Mater.* 49, 813 (2003).
14. A. Sharif, M.N. Islam, and Y.C. Chan, *Mater. Sci. Eng., B* 113, 184 (2004).
15. Y.C. Lin and J.G. Duh, *Scripta Mater.* 54, 1661 (2006).
16. Y.C. Lin, T.Y. Shih, S.K. Tien, and J.G. Duh, *Scripta Mater.* 56, 49 (2007).
17. N. Torazawa, S. Arai, Y. Takase, K. Sasaki, and H. Saka, *Mater. Trans.* 44, 1438 (2003).
18. H. Matsuki, H. Ibuka, and H. Saka, *Sci. Technol. Adv. Mater.* 3, 261 (2002).
19. V. Vuorinen, T. Laurila, H. Yu, and J.K. Kivilahti, *J. Appl. Phys.* 99, 023530 (2006).
20. C.W. Hwang, K. Suganuma, M. Kiso, and S. Hashimoto, *J. Mater. Res.* 18, 2540 (2003).
21. C.B. Lee, S.B. Jung, Y.E. Shin, and C.C. Shur, *Mater. Trans.* 43, 1858 (2002).
22. J.W. Yoon and S.B. Jung, *Mater. Sci. Forum.* 510–511, 554 (2006).
23. J.W. Jang, P.G. Kim, K.N. Tu, D.R. Frear, and P. Thompson, *J. Appl. Phys.* 85, 8456 (1999).
24. T.B. Massalski, *Binary Alloy Phase Diagrams* (Metals Park, OH: ASM International, 1987), pp. 2833–2837.